Electronic Supplementary Information (ESI):

for

Phase stability studies on transition metal phosphates aided by an automated synthesis

Stephanos Karafiludis[1,2*], Tom William Ryll[1,2], Ana G. Buzanich[1], Franziska Emmerling[1,2], and Tomasz M. Stawski[1*]

[1]Federal Institute for Materials Research and Testing, Richard Willstätter Str. 11 10249 Berlin, Germany

[2]Department of Chemistry, Humboldt-Universität zu Berlin, Brook-Taylor-Straße 2, 12489 Berlin

Stephanos Karafiludis: https://orcid.org/0000-0002-7257-6311;
Ana G. Buzanich: https://orcid.org/0000-0001-5543-9924 ;
Franziska Emmerling: https://orcid.org/0000-0001-8528-0301;
Tomasz M. Stawski: https://orcid.org/0000-0002-0881-5808;

Corresponding authors: *tomasz.stawski@bam.de;* stephanos.karafiludis@bam.de

List of Figures

List of Tables

Supplementary Note 1: Evaluation of automated synthesis and experimental error propagation

In automated synthesis, an assessment of possible sources of uncertainty should be considered. Due to the complex design of the Chemputer, a large number of mechanical parts such as tubes, valves, syringes, etc. could have an influence on the uncertainty of the concentrations used. In each synthesis, syringe pumps transport the chemicals from one chemical container into another. The accuracy of the pumps is given as ±0.1 ml for a volume of 10 ml, giving a relative uncertainty of 1%. Considering different tube lengths, the associated dead volumes would effectively reduce our reaction volume. Therefore, to solve this issue we implemented a pre-flushing of the tubes with 3 ml of a given solution in the synthesis procedure. As we always rinsed the system after each step, we were able to avoid any residual liquid throughout the synthesis. In the uncertainty propagation, we calculated the relative uncertainty in the synthesis of the stock solutions with 0.1% due to slight deviations in removing process of the solution and of the deionized water. For the dilution of each reactant solution, we determined the relative deviation to be 0.5% for most reactant concentrations, based on the differences in volume for the same reason as for the stock solution. Higher concentrations have a slightly higher relative uncertainty (0.7%) than lower concentrations (0.2%) as here the volume uncertainty contributes more to the absolute uncertainty. In a typical synthesis, the absolute volume uncertainty for a three-reactant synthesis is experimentally determined to be ±0.3 ml, which is 1% relative uncertainty for a reaction volume 30 ml. In the case of multicomponent synthesis with more than three reactants, a similar relative uncertainty can be expected, as the uncertainty of the syringe and of the two dilution steps would be low compared to the uncertainty propagation in a classical manual laboratory approach.

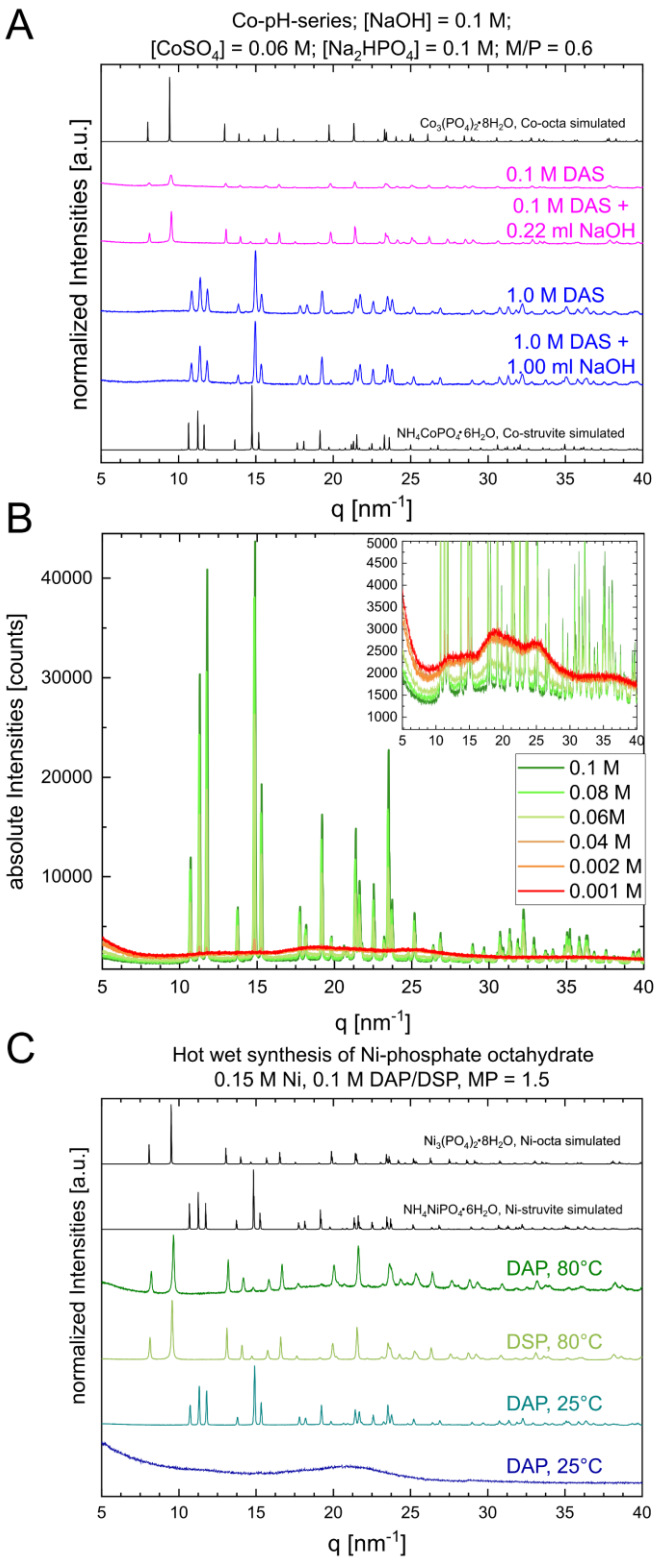

Figure S1: Diffractograms of (A) Co-phosphates synthesized at different pH. (B) Amorphous NH_4-series of Ni phosphate in absolute Intensities with detailed view of the background as inset and (C) Ni-phosphates synthesized at different temperatures (25°C and 80°C) and with different phosphate reactants (DAP = diammoniumphosphate $(NH_4)_2HPO_4$ or DSP = disodiumhydrogenphosphate Na_2HPO_4); Ni-struvite (NIS) reference database ICSD 403058; Co-struvite reference ICSD 170042; Ni-phosphate octahydrate ICSD 240946; Co-phosphate octahydrate COD 2020362.

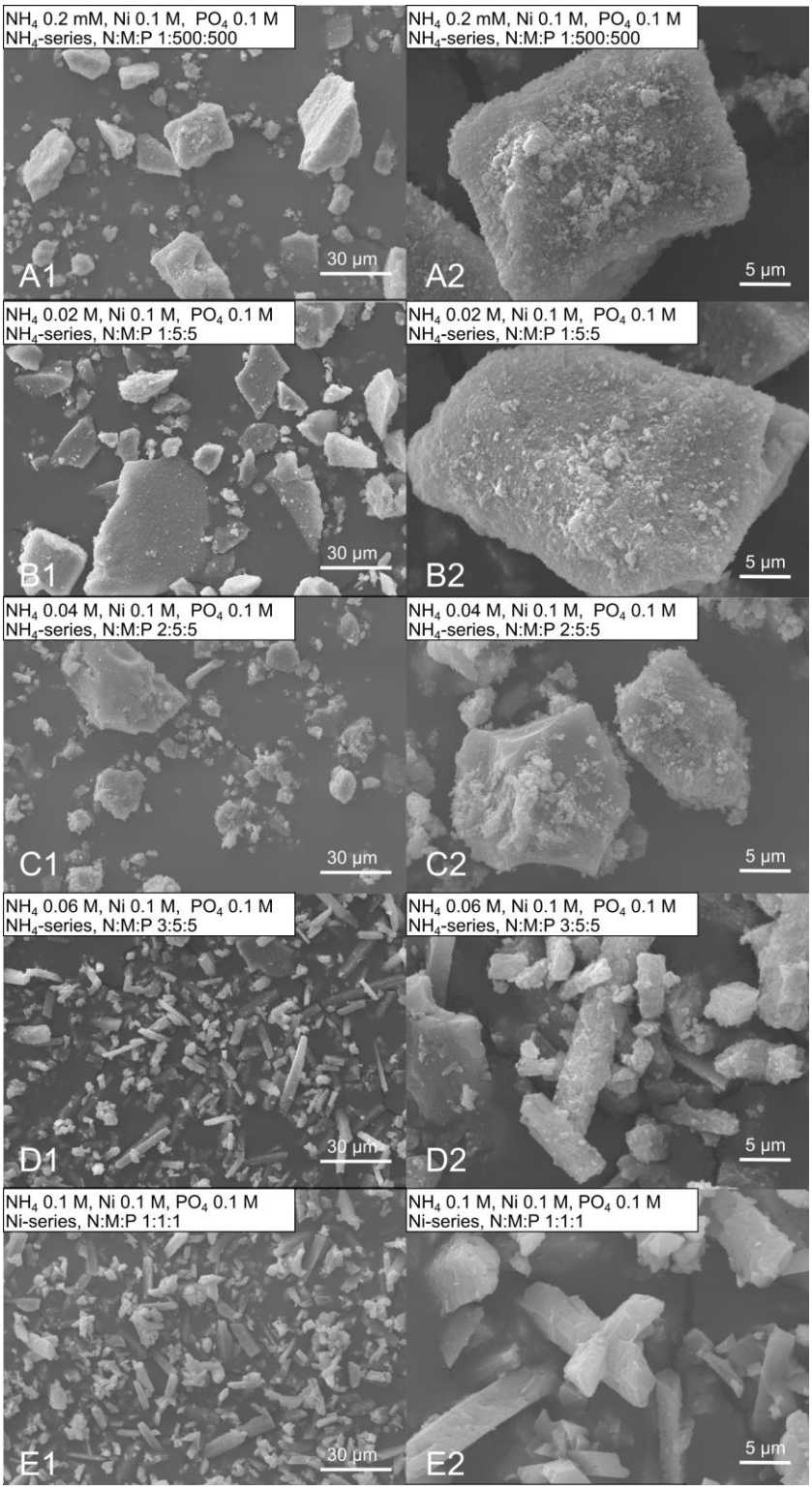

Figure S2: SE images of Ni-samples with an overview [30 µm] and more detailed photograph [5 µm] of the crystals/particles. The letters (A-I) are representative for a given reaction conditions, additionally described in the upper-left corner with the respective N:M:P ratio. The overview image is marked with 1 while the detailed photograph next to it is referred with 2. (A) 0.2 mM NH_4, 0.1 M Ni, 0.1 M PO_4; (B) 0.02 M NH_4, 0.1 M Ni, 0.1 M PO_4; (C) 0.04 M NH_4, 0.1 M Ni, 0.1 M PO_4; (D) 0.06 M NH_4, 0.1 M Ni, 0.1 M PO_4; (E) 0.1 M NH_4, 0.1 M Ni, 0.1 M PO_4; (F) 0.1 M NH_4, 0.02 M Ni, 0.1 M PO_4; (G) 0.1 M NH_4, 0.2 M Ni, 0.1 M PO_4; (H) 0.1 M NH_4, 0.1 M Ni, 0.02 M PO_4; (I) 0.1 M NH_4, 0.1 M Ni, 0.2 M PO_4.

Continuation of Figure S2 from the previous page.

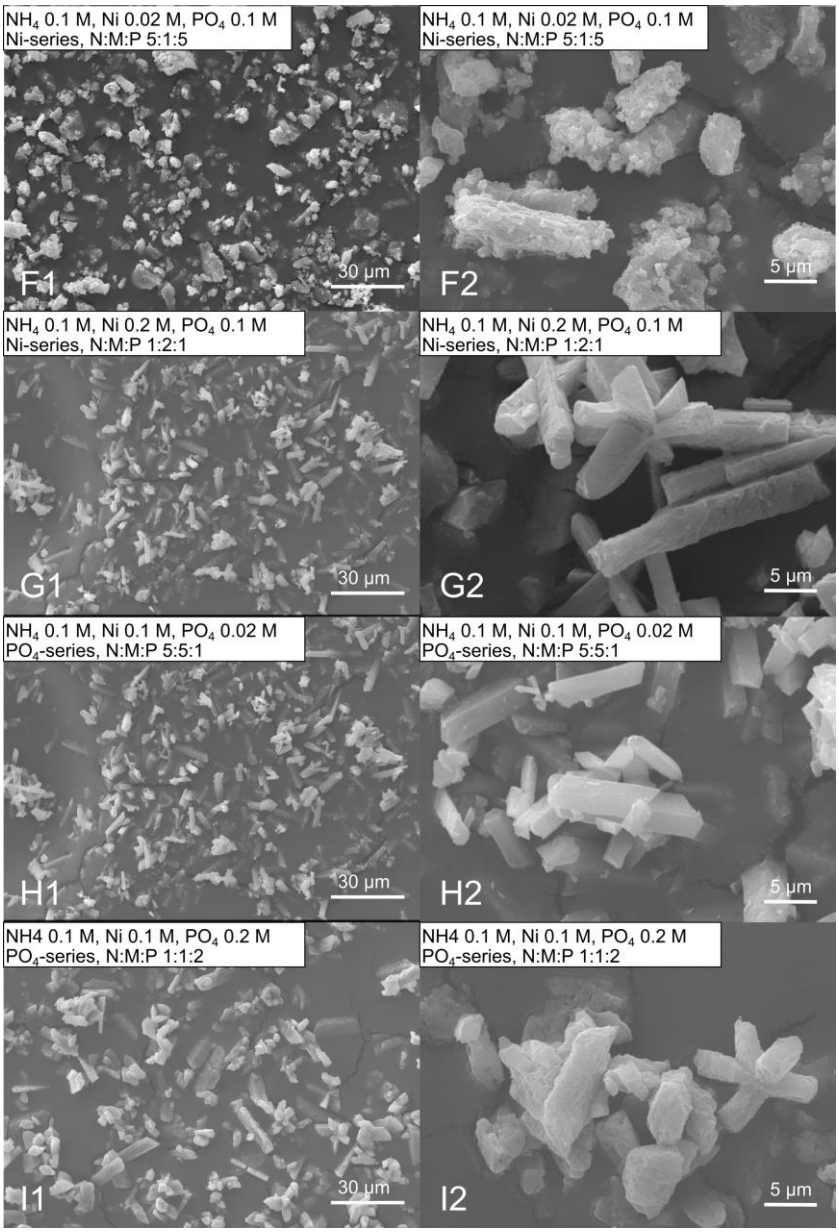

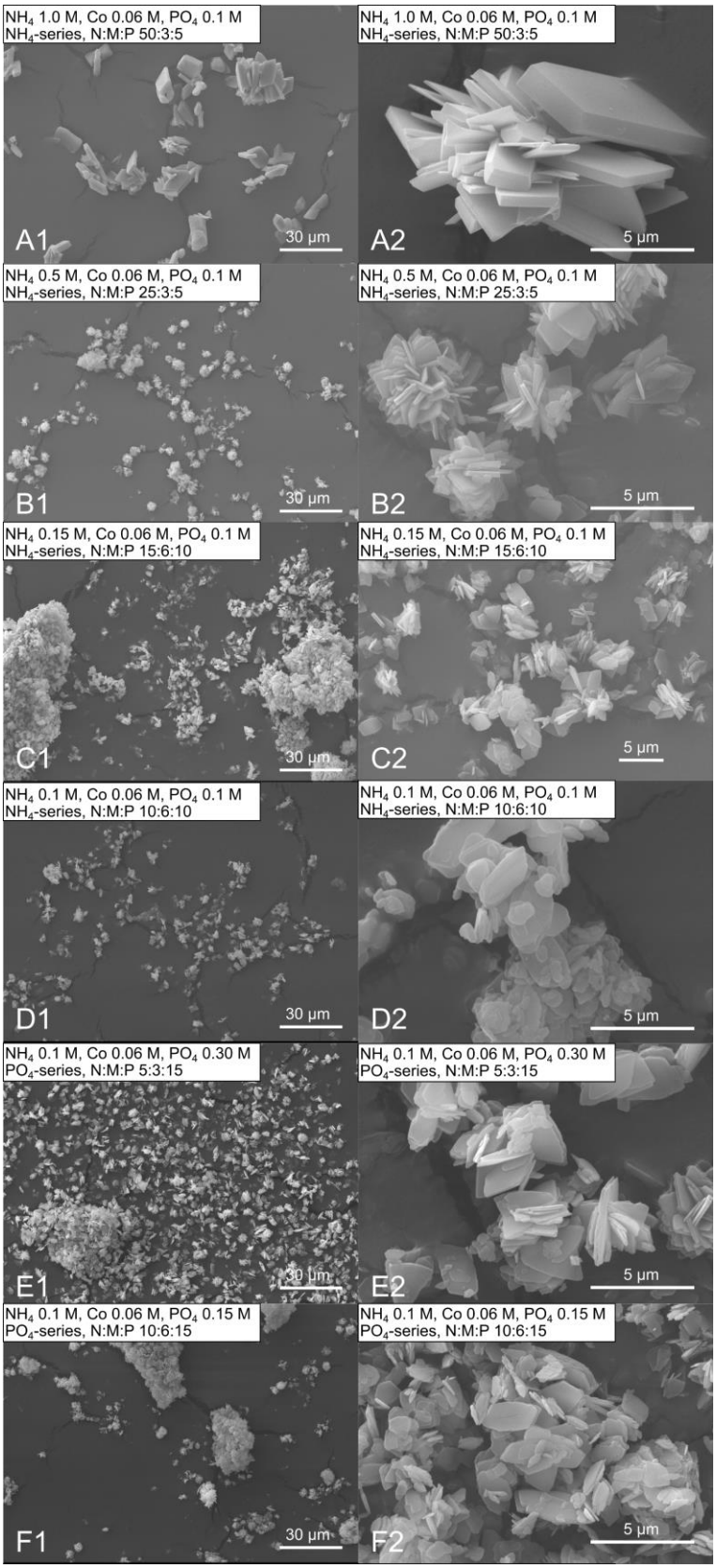

Figure S3: SE images of Co-samples with an overview [30 µm] and more detailed photograph [5 µm] of the crystals/particles. The letters (A-K) are representative for a given reaction conditions, additionally described in the upper-left corner with the respective N:M:P ratio. The overview image is marked with 1 while the detailed photograph next to it is referred with 2. (A) 1.0 M NH_4, 0.06 M Co, 0.1 M PO_4; (B) 0.5 M NH_4, 0.06 M Co, 0.1 M PO_4; (C) 0.15 M NH_4, 0.06 M Co, 0.1 M PO_4; (D) 0.1 M NH_4, 0.06 M Co, 0.1 M PO_4; (E) 0.1 M NH_4, 0.06 M Co, 0.3 M PO_4; (F) 0.1 M NH_4, 0.06 M Co, 0.15 M PO_4; (G) 0.1 M NH_4, 0.06 M Co, 0.08 M PO_4; (H) 0.1 M NH_4, 0.06 M Co,

0.06 M PO_4; (I) 0.1 M NH_4, 0.15 M Co, 0.1 M PO_4; (J) 0.1 M NH_4, 0.04 M Co, 0.1 M PO_4; (K) 0.1 M NH_4, 0.02 M Co, 0.1 M PO_4.

Continuation of Figure S3.

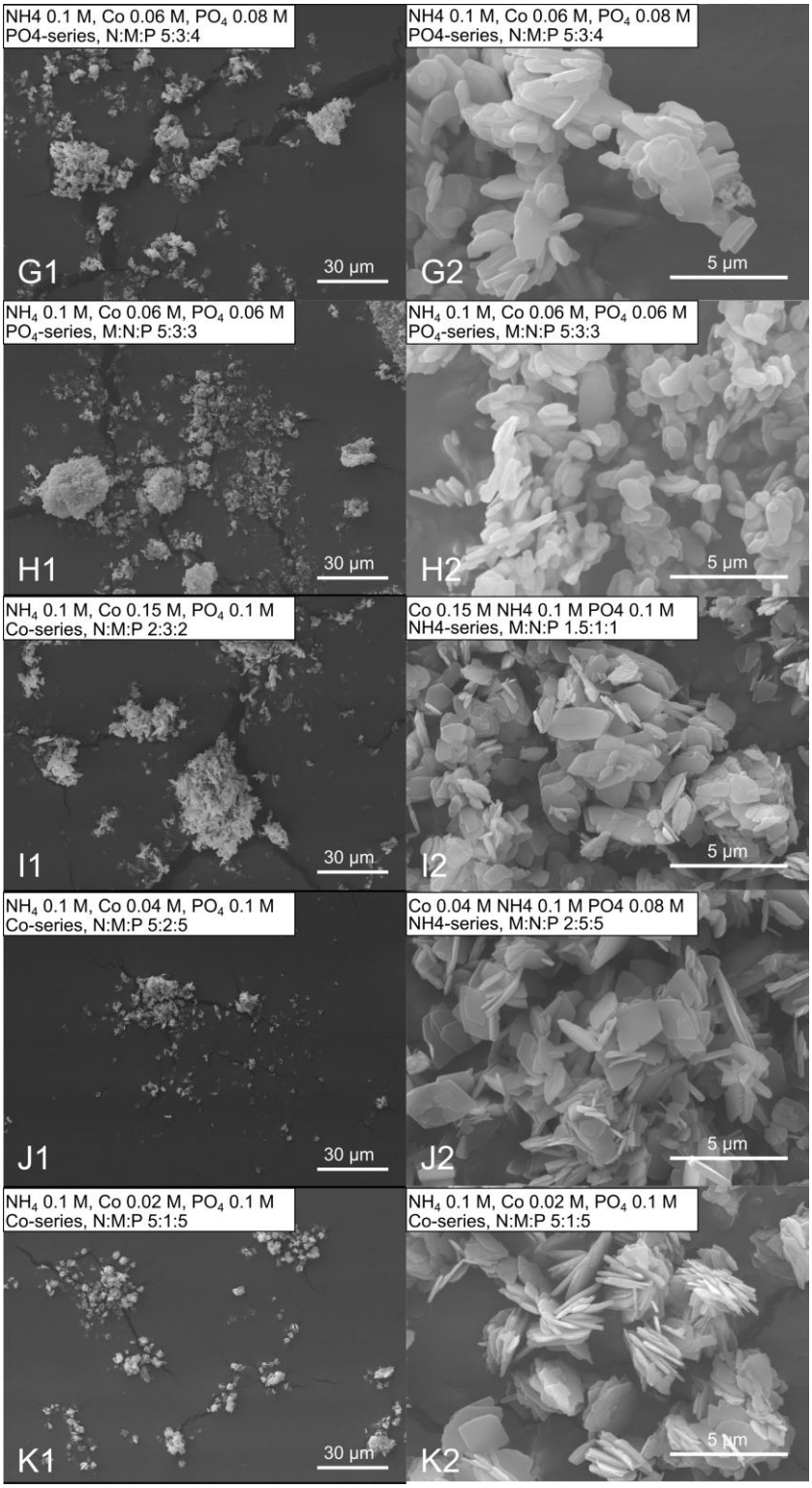

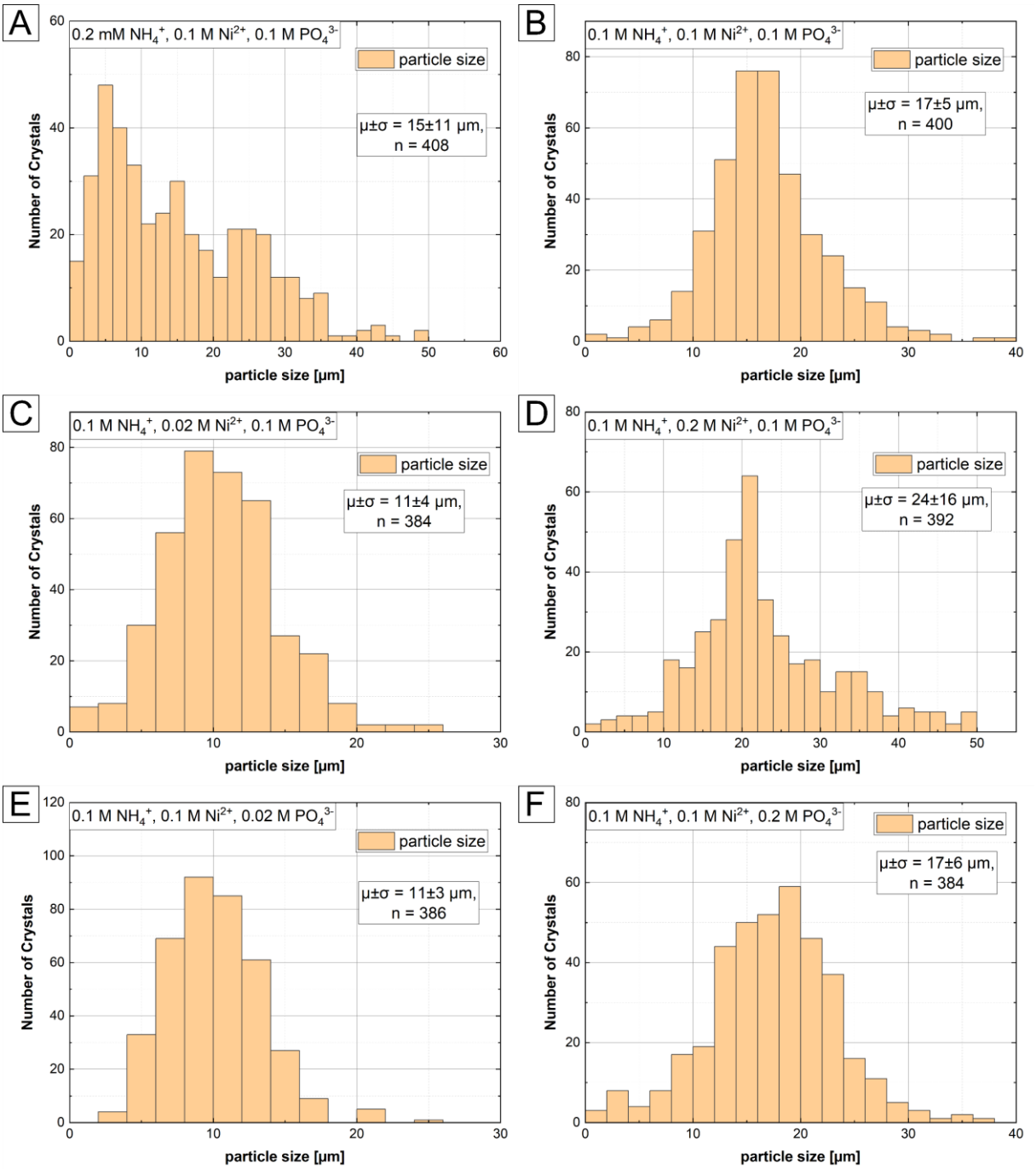

Figure S4: Exemplary size distribution histograms from selected Ni-samples (A) Histogram of 0.1 mM NH_4^+, 0.1 M Ni^{2+}, 0.1 M PO_4^{3-} with a total sample population of 408, μ ± σ = 15 ± 11 μm, (B) Histogram of 0.1 M NH_4^+, 0.1 M Ni^{2+}, 0.1 M PO_4^{3-} with a total sample population of 400, μ ± σ = 15 ± 5 μm, (C) Histogram of 0.1 M NH_4^+, 0.02 M Ni^{2+}, 0.1 M PO_4^{3-} with a total sample population of 384, μ ± σ = 11 ± 4 μm, (D) Histogram of 0.1 M NH_4^+, 0.2 M Ni^{2+}, 0.1 M PO_4^{3-} with a total sample population of 392, μ ± σ = 24 ± 16 μm, (E) Histogram of 0.1 M NH_4^+, 0.1 M Ni^{2+}, 0.02 M PO_4^{3-} with a total sample population of 386, μ ± σ = 11 ± 3 μm, (F) Histogram of 0.1 M NH_4^+, 0.1 M Ni^{2+}, 0.2 M PO_4^{3-} with a total sample population of 408, μ ± σ = 17 ± 6 μm.

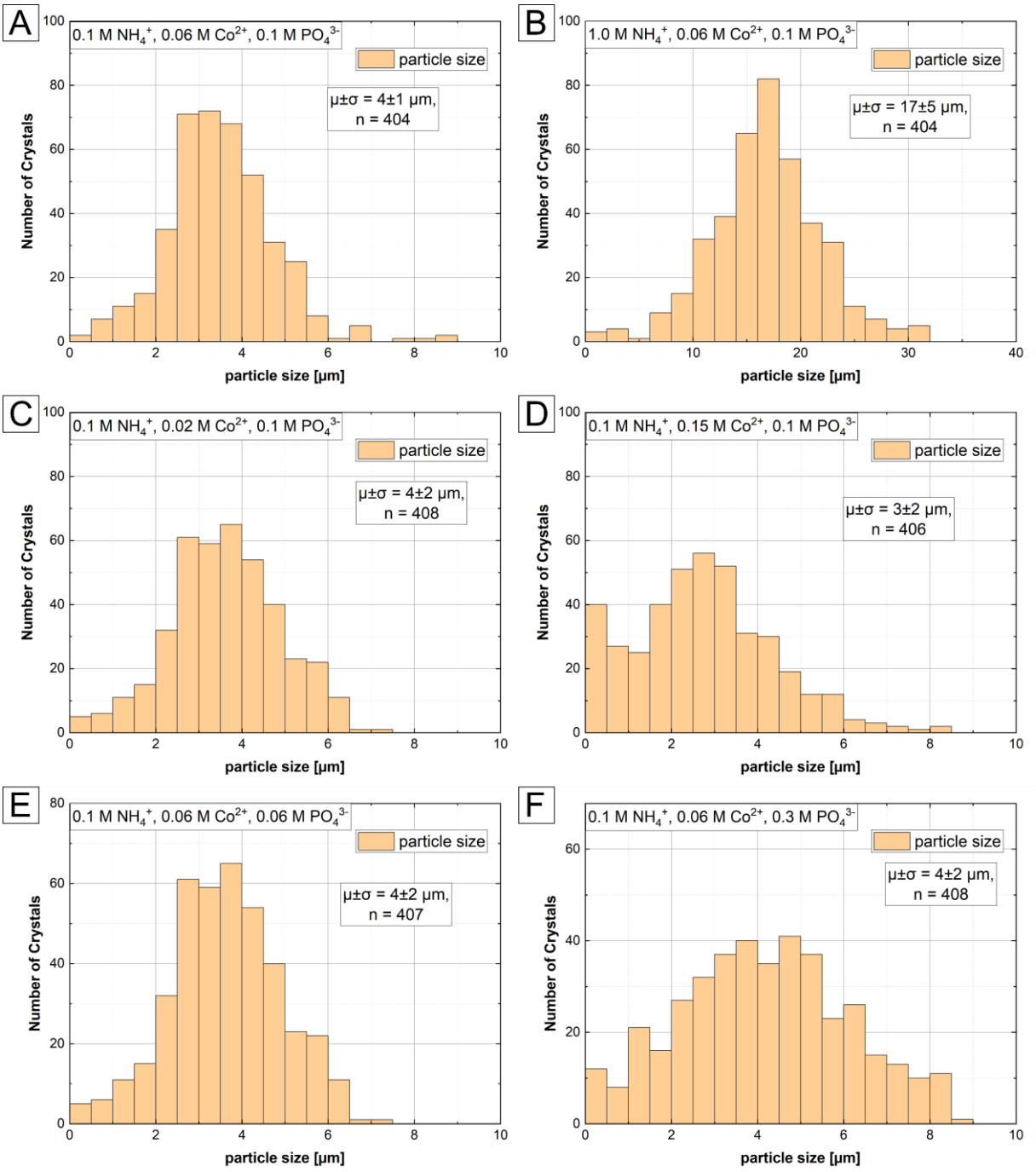

Figure S5: Exemplary size distribution histograms from selected Co-samples. (A) Histogram of 0.1 M NH_4^+, 0.06 M Co^{2+}, 0.1 M PO_4^{3-} with a total sample population of 404, $\mu \pm \sigma = 4 \pm 4$ µm, (B) Histogram of 1.0 M NH_4^+, 0.06 M Co^{2+}, 0.1 M PO_4^{3-} with a total sample population of 404, $\mu \pm \sigma = 17 \pm 5$ µm, (C) Histogram of 0.1 M NH_4^+, 0.02 M Co^{2+}, 0.1 M PO_4^{3-} with a total sample population of 408, $\mu \pm \sigma = 4 \pm 2$ µm, (D) Histogram of 0.1 M NH_4^+, 0.15 M Co^{2+}, 0.1 M PO_4^{3-} with a total sample population of 406, $\mu \pm \sigma = 3 \pm 2$ µm, (E) Histogram of 0.1 M NH_4^+, 0.06 M Co^{2+}, 0.06 M PO_4^{3-} with a total sample population of 407, $\mu \pm \sigma = 4 \pm 2$ µm, (F) Histogram of 0.1 M NH_4^+, 0.06 M Co^{2+}, 0.3 M PO_4^{3-} with a total sample population of 408, $\mu \pm \sigma = 4 \pm 2$.

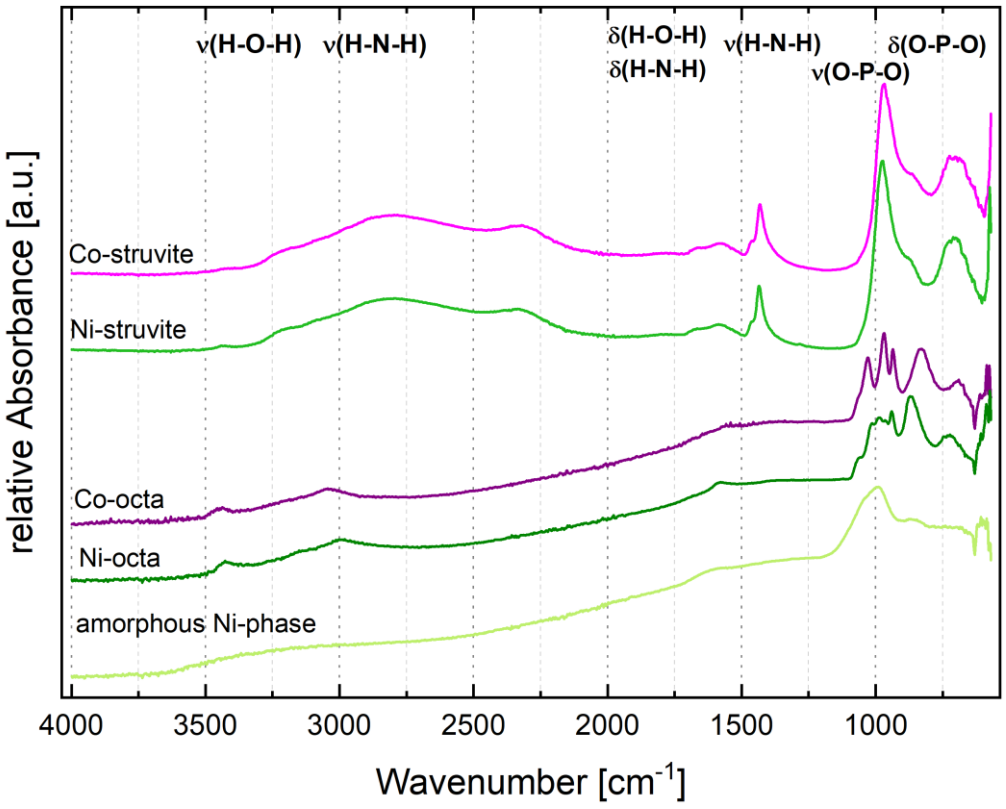

Figure S6: Fourier transformed-infrared (FT-IR) spectra of crystalline Ni-, Co- struvite and phosphate octahydrate in juxtaposition with the amorphous Ni-PO_4 phase.

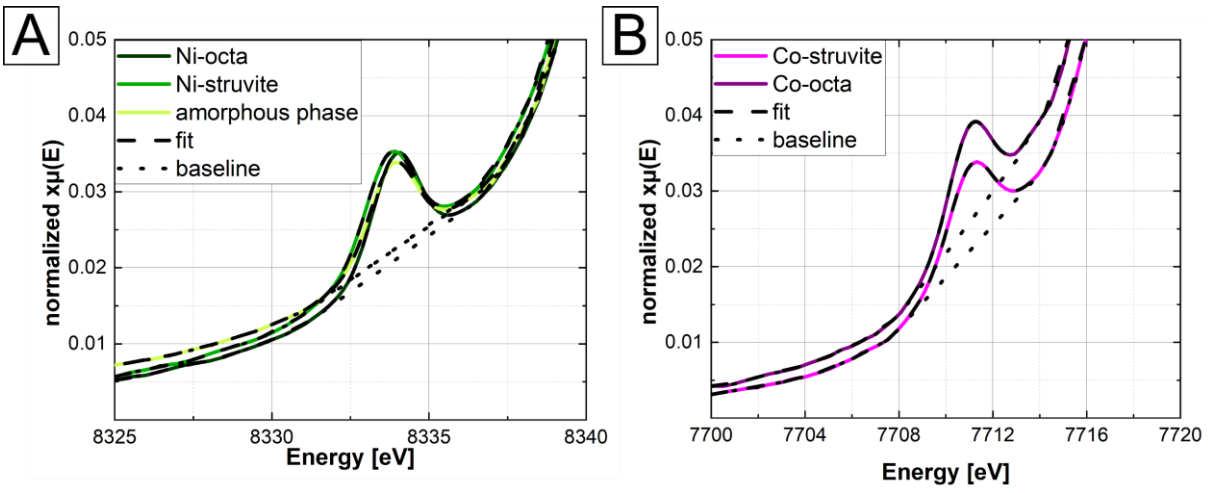

Figure S7: XANES spectra of pre-peak region, integration of Gaussian fits and associated baselines for (A) Ni-phosphates and (B) Co-phosphates.

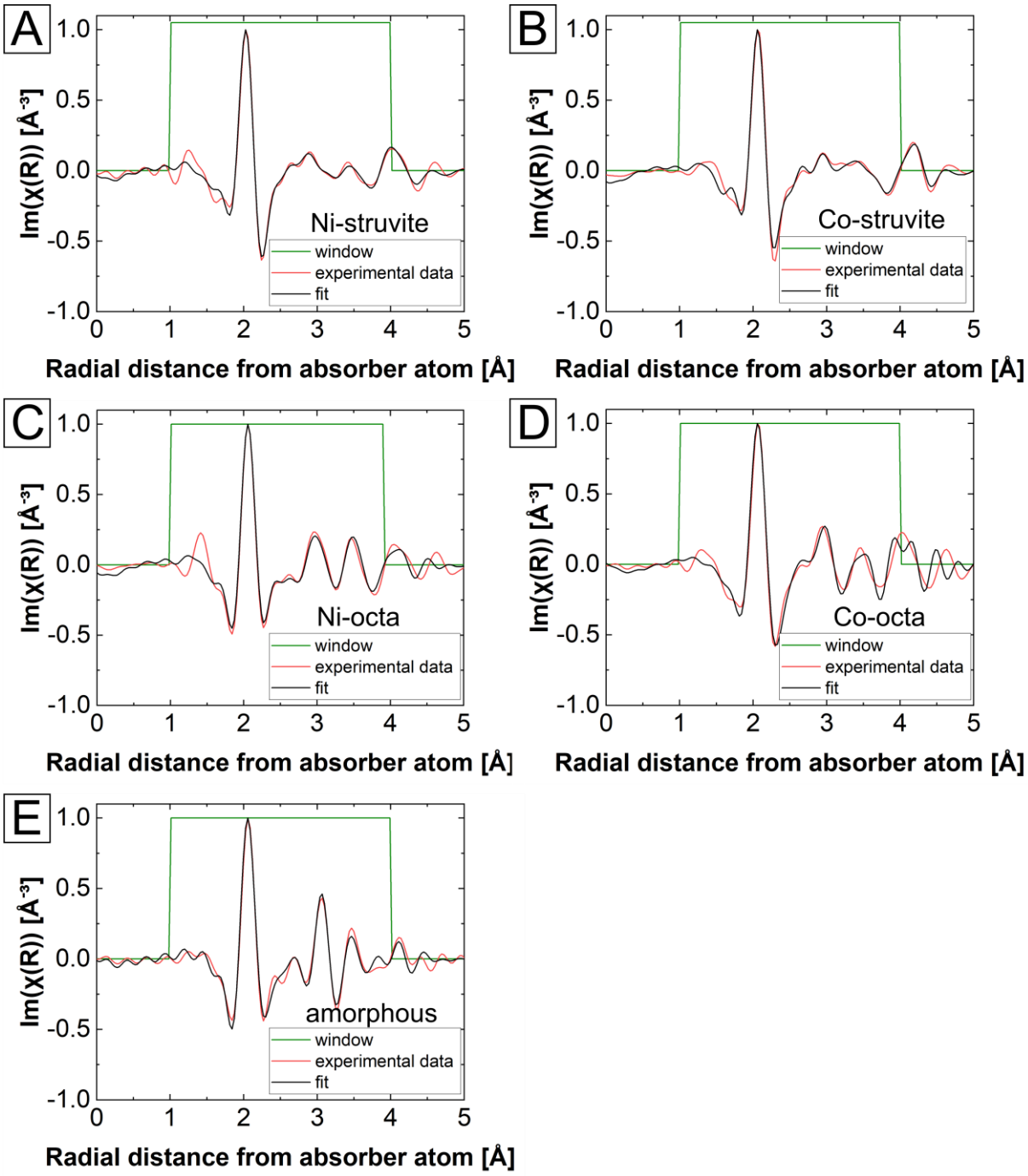

Figure S8: Ni- and Co-K-edge EXAFS data and fits shown in imaginary space for (A) Ni-struvite $NH_4NiPO_4 \cdot 6H_2O$ with R-factor = 0.014, (B) Co-struvite $NH_4CoPO_4 \cdot 6H_2O$ with R = 0.014, (C) Ni-phosphate octahydrate $Ni_3(PO_4)_2 \cdot 8H_2O$ with R = 0.014, (D) Co-phosphate octahydrate $Co_3(PO_4)_2 \cdot 8H_2O$ with R = 0.013 and (E) amorphous Ni-PO_4 phase with R = 0.018.

Table S1: Calculated pre-peak integration results [R^2, integrated area A_{pp}, Full Width Half Maximum (FWHM), centre of the peak and maximum height] from the pre-peak region of Ni- and Co-Phosphate samples with their respective chemical composition. The distinct peak was fitted by a Gaussian model and then integrated over this region. The calculated pre-peak area values A_{pp} represent more semi-quantitative and are of a comparative purpose rather than show absolute values.

Pre-peak area integration results				fit function: Gaussian		
Sample	chemical formula	R^2 value	Pre-peak Area A_{pp} (err)	FWHM	Center	Max. Height
Ni-struvite	$NH_4NiPO_4 \cdot 6H_2O$	0.998	0.025(2)	1.80	8333.8	0.013
Ni-phosphate octahydrate	$Ni_3(PO_4)_2 \cdot 8H_2O$	0.999	0.030(1)	1.69	8334	0.014
amorphous Ni-PO_4	Ni-PO_4	0.997	0.024(2)	1.67	8333.8	0.013
Co-struvite	$NH_4CoPO_4 \cdot 6H_2O$	0.996	0.027(1)	2.17	7711.1	0.011
Co-phosphate octahydrate	$Co_3(PO_4)_2 \cdot 8H_2O$	0.994	0.035(2)	2.05	7711	0.013

Table S2: Fit parameter for the amorphous Ni-PO_4 phase, R-factor= 0.018.

Sample	scattering path	N	σ^2	R_{diff} [Å]	R_{diff}^2 [Å^2]	R_{model} [Å]	R_{fit} [Å]
amorphous	Ni1-O1	2	0.005	-2.58E-02	6.63E-04	2.030	2.004
Ni-PO_4	Ni1-O2	4	0.005	-2.58E-02	6.63E-04	2.105	2.079
	Ni1-H1	4	0.003	-6.15E-02	3.78E-03	2.502	2.440
R-factor	Ni1-H2	4	0.003	-6.15E-02	3.78E-03	2.549	2.487
0.018	Ni1-P1	2	0.000	2.56E-02	6.54E-04	3.189	3.214
S_O^2 (err)	Ni1-O3	4	0.003	-6.15E-02	3.78E-03	3.567	3.506
0.89(9)	Ni1-O4	2	0.003	-6.15E-02	3.78E-03	3.621	3.559
ΔE	Ni1-O5	2	0.003	-6.15E-02	3.78E-03	3.941	3.879
-1.7(8)	Ni1-O6-H3	16	-0.005	-2.72E-01	7.40E-02	4.003	3.731
	Ni1-O3-O7	8	-0.005	-2.72E-01	7.40E-02	4.051	3.778
	Ni1-O7-O7	2	-0.005	-2.72E-01	7.40E-02	4.060	3.788
	Ni1-O8	2	0.003	-6.15E-02	3.78E-03	4.060	3.999
	Ni1-O9	4	0.003	-6.15E-02	3.78E-03	4.461	4.399

Table S3: Fit parameter for Ni-phosphate octahydrate $Ni_3(PO_4)_2 \cdot 8H_2O$, R-factor= 0.014.

Sample	scattering path	N	σ^2	R_{diff} [Å]	R_{diff}^2 [Å^2]	R_{model} [Å]	R_{fit} [Å]
Ni-octa	Ni1-O1	4	0.007	-1.01E-02	1.01E-04	2.062	2.059
$Ni_3(PO_4)_2 \cdot 8H_2O$	Ni1-O2	2	0.007	-1.01E-02	1.01E-04	2.097	2.094
	Ni1-H1	4	0.009	-9.06E-02	8.20E-03	2.517	2.427
R-factor	Ni1-Ni2	2	0.016	4.51E-02	2.04E-03	2.909	2.962
0.014	Ni1-P1	3	0.016	4.51E-02	2.04E-03	3.220	3.274
S_O^2 (err)	Ni1-O3	2	0.009	-9.06E-02	8.20E-03	3.449	3.360
1.1(1)	Ni1-P2	2	0.016	4.51E-02	2.04E-03	3.319	3.372
ΔE	Ni1-O4	2	0.009	-9.06E-02	8.20E-03	3.521	3.432
-0.7(9)	Ni1-O5	2	0.009	-9.06E-02	8.20E-03	3.882	3.793
	Ni1-O6	2	0.009	-9.06E-02	8.20E-03	3.932	3.843
	Ni1-O7	2	0.009	-9.06E-02	8.20E-03	3.992	3.903
	Ni1-O8	4	0.009	-9.06E-02	8.20E-03	4.034	3.944
	Ni1-O9	2	0.009	-9.06E-02	8.20E-03	4.137	4.048
	Ni1-O10	16	0.017	-1.38E-02	1.91E-04	4.460	4.455

Table S4: Fit parameter for Co-phosphate octahydrate $Co_3(PO_4)_2 \cdot 8H_2O$, R-factor= 0.013.

Sample	scattering path	N	σ^2	R_{diff} [Å]	R_{diff}^2 [Å^2]	R_{model} [Å]	R_{fit} [Å]
Co-octa	Ni1-O1	4	0.008	4.61E-02	2.13E-03	2.021	2.068
$Co_3(PO_4)_2 \cdot 8H_2O$	Ni1-O2	2	0.008	4.61E-02	2.13E-03	2.158	2.204
	Ni1-H1	4	0.012	-6.19E-02	3.83E-03	2.451	2.389
R-factor	Ni1-O2-H2	8	-0.002	4.28E-01	1.83E-01	2.593	3.021
0.013	Ni1-P1	2	0.012	2.21E-02	4.86E-04	3.194	3.216
S_O^2 (err)	Ni1-H3	4	0.012	-6.19E-02	3.83E-03	3.226	3.164
1.2(1)	Ni1-H4	8	0.012	-6.19E-02	3.83E-03	3.319	3.257
ΔE	Ni1-P1-O2	4	0.021	1.77E-02	3.14E-04	3.389	3.406
4.3(7)	Ni1-O1-O2	8	0.021	1.77E-02	3.14E-04	3.553	3.570
	Ni1-O3	4	0.012	-6.19E-02	3.83E-03	3.579	3.517
	Ni1-O1-O3	8	0.021	1.77E-02	3.14E-04	3.584	3.602
	Ni1-O4	2	0.012	-6.19E-02	3.83E-03	3.675	3.613
	Ni1-O2-O2	8	0.021	1.77E-02	3.14E-04	3.684	3.702
	Ni1-O5	8	0.012	-6.19E-02	3.83E-03	3.950	3.888
	Ni1-H4-O5	16	-0.002	4.28E-01	1.83E-01	4.014	4.442

Table S5: Fit parameter for Ni-struvite $NH_4NiPO_4 \cdot 6H_2O$, R-factor= 0.014.

Sample	scattering	N	σ^2	R_{diff} [Å]	R_{diff}^2	R_{model}	R_{fit}
Ni-struvite	Ni1-O1	4	0.008	-3.97E-03	1.58E-05	2.046	2.042
$NH_4NiPO_4 \cdot 6H_2O$	Ni1-O2	2	0.008	-3.97E-03	1.58E-05	2.089	2.085
	Ni1-H1	4	0.001	-2.11E-01	4.46E-02	2.560	2.349
R-factor	Ni1-H2	5	0.014	-2.18E-01	4.76E-02	2.586	2.368
0.014	Ni1-H3	2	0.014	-2.18E-01	4.76E-02	2.627	2.409
S_O^2 (err)	Ni1-H4	2	0.014	-2.18E-01	4.76E-02	2.668	2.450
1.3(1)	Ni1-O1-O1	6	0.001	-2.11E-01	4.46E-02	3.465	3.254
ΔE	Ni1-O2-O3	16	0.001	-2.11E-01	4.46E-02	3.530	3.318
2.9(7)	Ni1-Ni2	2	0.004	-2.18E-01	4.74E-02	4.111	3.893
	Ni1-O4	4	0.005	2.45E-01	5.98E-02	4.084	4.329
	Ni1-O5	2	0.005	2.45E-01	5.98E-02	4.162	4.406
	Ni1-O6	2	0.005	2.45E-01	5.98E-02	4.200	4.444
	Ni1-O7	3	0.005	2.45E-01	5.98E-02	4.272	4.517
	Ni1-O8	2	0.005	2.45E-01	5.98E-02	4.329	4.574

Table S6: Fit parameter for Co-struvite $NH_4CoPO_4 \cdot 6H_2O$, R-factor= 0.014.

Sample	scattering path	N	σ^2	R_{diff} [Å]	R_{diff}^2 [Å^2]	R_{model} [Å]	R_{fit} [Å]
Co-struvite	Ni1-O1	2	0.007	-8.00E-03	6.40E-05	2.058	2.050
$NH_4CoPO_4 \cdot 6H_2O$	Ni1-O2	2	0.007	-8.00E-03	6.40E-05	2.089	2.081
	Ni1-O3	2	0.007	-8.00E-03	6.40E-05	2.129	2.121
R-factor	Ni1-H5	2	0.003	-9.42E-02	8.87E-03	2.616	2.522
0.014	Ni1-H1	2	0.002	3.20E-01	1.02E-01	2.211	2.531
S_O^2 (err)	Ni1-H2	2	0.002	3.20E-01	1.02E-01	2.451	2.771
1.0(1)	Ni1-H3	1	0.002	3.20E-01	1.02E-01	2.507	2.826
ΔE	Ni1-H4	4	0.002	3.20E-01	1.02E-01	2.549	2.869
3.2(6)	Ni1-N1	1	0.003	-9.42E-02	8.87E-03	4.027	3.932
	Ni1-N2	2	0.003	-9.42E-02	8.87E-03	4.133	4.038
	Ni1-O4	4	0.001	3.48E-01	1.21E-01	4.105	4.453
	Ni1-O5	4	0.001	3.48E-01	1.21E-01	4.199	4.547
	Ni1-O6	3	0.001	3.48E-01	1.21E-01	4.288	4.636
	Ni1-O7	1	0.001	3.48E-01	1.21E-01	4.362	4.710